

# Creation of superposition of arbitrary states encoded in two three-dimensional cavities

Tong Liu<sup>1</sup>, Yang Zhang<sup>2</sup>, Bao-qing Guo<sup>1</sup>, Chang-shui Yu<sup>1\*</sup>, and Wei-ning Zhang<sup>1</sup>

<sup>1</sup>*School of Physics, Dalian University of Technology, Dalian 116024, China and*

<sup>2</sup>*Institute of Theoretical Physics, Shanxi Datong University, Datong 037009, China*

(Dated: December 15, 2024)

The principle of superposition is a key ingredient for quantum mechanics. A recent work [M. Oszmaniec *et al.*, Phys. Rev. Lett. 116, 110403 (2016)] has shown that a quantum adder that deterministically generates a superposition of two unknown states is forbidden. Here we propose a probabilistic approach for creating a superposition state of two arbitrary states encoded in two three-dimensional cavities. Our implementation is based on a three-level superconducting transmon qubit dispersively coupled to two cavities. Numerical simulations show that high-fidelity generation of the superposition of two coherent states is feasible with current circuit QED technology. Our method also works for other physical systems such as other types of superconducting qubits, natural atoms, quantum dots, and nitrogen-vacancy (NV) centers.

PACS numbers: 03.67.Lx, 42.50.Pq, 85.25.Cp, 42.50.Dv

## I. INTRODUCTION

The superpositions of quantum states is at the heart of the basic postulates and theorems of quantum mechanics. Quantum superposition studies the application of quantum theory or phenomena, that is different from the classical world, leads to many other intriguing quantum phenomena such as quantum entanglement [1] and quantum coherence [2, 3]. It is a vital physical resource and has many important applications in quantum information processing (QIP) and quantum computation such as quantum algorithms [4, 5], quantum metrology [6], and quantum cryptography [7].

A quantum adder is a quantum machine adding two arbitrary unknown quantum states of two different systems onto a single system [8, 9]. How to generate a superposition of two arbitrary states has recently aroused great interest in the field of quantum optics and quantum information. For example, Refs. [8, 9] have proved that it is impossible to generate a superposition of two unknown states, but Ref. [9] proposed a method to probabilistically creating the superposition of two known pure states with the fixed overlaps. Ref. [10] has shown that superpositions of orthogonal qubit states can be produced with unit probability, and Ref. [11] has demonstrated that the state transfer can be protected via an approximate quantum adder. Recently, the probabilistic creation of superposition of two unknown quantum states has been demonstrated experimentally in linear optics [12] and nuclear magnetic resonance (NMR) [13].

Circuit quantum electrodynamics (QED) consisting of superconducting qubits and microwave cavities are now moving toward multiple superconducting qubits, multiple three-dimensional (3D) cavities with greatly enhanced coherence time, making them particularly appealing for large-scale quantum computing [14–16]. For example,

a 3D microwave cavity with the photon lifetime up to 2  $s$  [17] and a transmon with a coherence time  $\sim 0.1 ms$  [18] have been recently reported in 3D circuit QED. Hence, 3D cavities are good memory elements, which can have coherence time at least four orders of magnitude longer than the transmons. By encoding quantum information in microwave cavities, many schemes have been proposed for synthesizing Bell states [19], NOON states [20–26], and entangled coherent states [27, 28] of multiple cavities, and realizing cross-Kerr nonlinearity interaction between two cavities [29, 30].

Three-dimensional circuit QED has emerged as a well-established platform for quantum information processing (QIP) and quantum computation [31–36], including creation of a Schrödinger cat state of a microwave cavity [32], preparation and control of a five-level transmon qudit [33], demonstration of a quantum error correction [34], realization of a two-mode cat state of two microwave cavities [35], and implementation of a controlled-NOT gate between multiphoton qubits encoded in two cavities [36]. Considering these advancements in 3D circuit QED, it is quite meaningful and necessary to implement a quantum adder in such systems.

In this paper, we present a probabilistic scheme to realize a quantum adder that creates a superposition of two unknown states by using a superconducting transmon qubit dispersively coupled to two 3D cavities. This circuit architecture has been experimentally demonstrated recently in [35]. Our protocol has the following features and advantages: (i) The superposition of two states are encoded in two three-dimensional cavities which have long coherence time rather than encoded in qubits. (ii) The states of cavities can be in arbitrary states, e.g., discrete-variable states or continuous-variable states. (iii) Due to the interaction between the two cavities is mediated by the transmon, cavity-induced dissipations are greatly suppressed. (iv) Our proposal can also be applied to other physical systems such as quantum dot-cavity system [37], natural atom-cavity system [38], superconducting circuits with other types of su-

---

\*Corresponding author: ycs@dlut.edu.cn

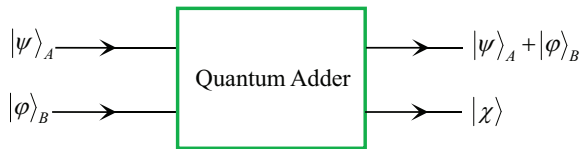


FIG. 1: (color online) A diagram of the quantum adder. Here,  $|\psi\rangle_a$  and  $|\varphi\rangle_b$  are the two arbitrary input pure states, while  $|\psi\rangle_a + |\varphi\rangle_b$  is the out superposition state with the referential state  $|\chi\rangle$ .

perconducting qubits (e.g., phase qubit [39], Xmon qubit [40], flux qubit [41]), hybrid circuits for two nitrogen-vacancy center ensembles coupled to a single flux qubit [42].

The structure of this paper is as follows. In Sec. II, we review some basic theory of quantum adder that creates the superposition of two arbitrary states. Our experimental system and Hamiltonian are introduced in Sec. III. In Sec. IV, we show a method to implement a quantum adder in 3D circuit QED system. In Sec. V, we give a brief discussion on the experimental implementation of a quantum adder with state-of-the-art circuit QED technology. Finally, Sec. VI gives a brief concluding summary.

## II. BASIC THEORY OF QUANTUM ADDER

We now review some basic theory of quantum adder (Fig. 1) which can generate the superposition of two pure states. Assume that particles  $A$  and  $B$  are respectively initially in arbitrary pure states  $|\psi\rangle_A$  and  $|\varphi\rangle_B$ , and an ancilla particle  $T$  is prepared in an arbitrary superposition state  $|\phi\rangle_T = \alpha|0\rangle_T + \beta|1\rangle_T$  with normalized coefficients  $\alpha$  and  $\beta$ . We first implement a three-qubit controlled-SWAP gate such that the initial state  $|\psi\rangle_A|\varphi\rangle_B|\phi\rangle_T$  of three qubits evolves into

$$\alpha|\psi\rangle_A|\varphi\rangle_B|0\rangle_T + \beta|\varphi\rangle_A|\psi\rangle_B|1\rangle_T, \quad (1)$$

where the qubit  $T$  is a control qubit and qubits  $A$  and  $B$  are two target qubits. Equation (1) means that the states of the target qubits are swapped only if the the control qubit is in the state  $|1\rangle$  and unchanged otherwise.

Then we make projective measurements on the states  $|\pm\rangle_T$  and  $|\chi\rangle_B$  of qubits  $T$  and  $A$ , respectively. Here,  $|\pm\rangle_T = (|1\rangle_T \pm |0\rangle_T)/\sqrt{2}$  and  $|\chi\rangle_B$  is the referential state which satisfies  $\langle\chi|\psi\rangle_B \neq 0$  and  $\langle\chi|\varphi\rangle_B \neq 0$ . Accordingly, one obtains the following superposition state of qubit  $A$

$$|\Psi\rangle_A = \frac{1}{N}(\gamma|\psi\rangle + \eta|\varphi\rangle), \quad (2)$$

where  $\gamma = \alpha\langle\chi|\varphi\rangle_B$ ,  $\eta = \beta\langle\chi|\psi\rangle_B$ , and the normalization constant  $N = \sqrt{2[|\gamma|^2 + |\eta|^2 + 2\text{Re}(\gamma\eta^*\langle\varphi|\psi\rangle)]}$ . As shown in above operations, the superposition state of

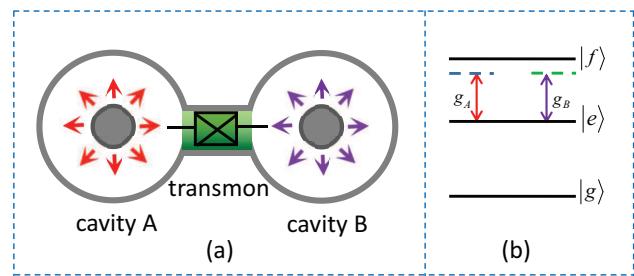


FIG. 2: (color online) (a) Schematic of a single transmon qubit dispersively coupled to two three-dimensional microwave cavities  $A$  and  $B$ . (b) Schematic representation of level configuration of the transmon. The cavities  $A$  and  $B$  are off-resonantly coupled to the  $|e\rangle \leftrightarrow |f\rangle$  transition of the transmon with coupling strengths  $g_A$  and  $g_B$ , respectively.

Eq. (2) can be produced under the knowledge about the overlaps  $\langle\chi|\varphi\rangle$  and  $\langle\chi|\psi\rangle$ . We find that if we vary the coefficients  $\alpha$  and  $\beta$ , then the arbitrary superposition state of qubit  $A$  is prepared with prior knowledge of the overlaps.

## III. SYSTEM AND HAMILTONIAN

Motivated by the experimental advances in 3D circuit QED, we here consider a circuit system consisting of a transmon qubit (with three states  $|g\rangle$ ,  $|e\rangle$  and  $|f\rangle$ ) capacitively coupled to two separate 3D superconducting cavities as shown in Fig. 2. We start with the following Hamiltonian to describe the microwave cavities are coupled to the  $|e\rangle \leftrightarrow |f\rangle$  transition of transmon:  $H = H_0 + H_I$ . When setting  $\hbar = 1$ , the Hamiltonian  $H_0$  is written as

$$H_0 = \omega_{eg}|e\rangle\langle e| + (\omega_{eg} + \omega_{fe})|f\rangle\langle f| + \omega_A a^\dagger a + \omega_B b^\dagger b, \quad (3)$$

where  $\omega_{eg}$  ( $\omega_{fe}$ ) is the  $|g\rangle \leftrightarrow |e\rangle$  ( $|e\rangle \leftrightarrow |f\rangle$ ) transition frequency of transmon qubit,  $\omega_A$  ( $\omega_B$ ) is the frequency of cavity  $A$  ( $B$ ), and  $a^\dagger$  and  $a$  ( $b^\dagger$  and  $b$ ) are the creation and annihilation operators for cavity  $A$  ( $B$ ).

The coupling Hamiltonian  $H_I$  of the whole system is given by

$$H_I = g_A(a\sigma_{fe}^+ + a^\dagger\sigma_{fe}^-) + g_B(b\sigma_{fe}^+ + b^\dagger\sigma_{fe}^-), \quad (4)$$

where  $\sigma_{fe}^+ = |f\rangle\langle e|$  ( $\sigma_{fe}^- = |e\rangle\langle f|$ ) represents qubit raising (lowering) operator and  $g_A$  ( $g_B$ ) denotes the qubit-cavity coupling strength.

The effective Hamiltonian can be deduced in the dispersive regime  $|\Delta_j| = |\omega_{fe} - \omega_j| \gg g_j$  ( $j = A, B$ ) using the Fröhlich-Nakajima transformation. We first find that an anti-Hermitian operator  $V$  (i.e.,  $V = -V^\dagger$ ) such that it satisfies

$$H_I + [H_0, V] = 0. \quad (5)$$

By making the unitary transformation  $U = \exp(-V)$  to  $H$  and expanding to second order in the couplings, we can obtain the following effective Hamiltonian

$$H_e = U^\dagger H U = H_0 + \frac{1}{2}[H_I, V], \quad (6)$$

where we set the anti-Hermitian operator

$$V = \frac{g_A}{\Delta_A} \left( a^\dagger \sigma_{fe}^- - a \sigma_{fe}^+ \right) + \frac{g_B}{\Delta_B} \left( b^\dagger \sigma_{fe}^- - b \sigma_{fe}^+ \right). \quad (7)$$

On substituting Eqs. (3), (4) and (7) into Eq. (6), one obtains

$$\begin{aligned} H_e = & \omega_{eg}|e\rangle\langle e| + (\omega_{eg} + \omega_{fe})|f\rangle\langle f| \\ & + \omega_A a^\dagger a + \omega_B b^\dagger b \\ & + \left( \frac{g_A^2}{\Delta_A} a a^\dagger + \frac{g_B^2}{\Delta_B} b b^\dagger \right) |f\rangle\langle f| \\ & - \left( \frac{g_A^2}{\Delta_A} a^\dagger a + \frac{g_B^2}{\Delta_B} b^\dagger b \right) |e\rangle\langle e| \\ & + \mu(a^\dagger b + a b^\dagger)(|f\rangle\langle f| - |e\rangle\langle e|), \end{aligned} \quad (8)$$

with  $\mu = \frac{g_A g_B}{2} \left( \frac{1}{\Delta_A} + \frac{1}{\Delta_B} \right)$  corresponding to the effective coupling strength. This effective coupling strength can be adjusted by the couplings  $g_A$ ,  $g_B$  and the detunings  $\Delta_A$  and  $\Delta_B$ . Notice that the third and fourth lines of Eq. (8) describe Stark shifts of the levels  $|f\rangle$  and  $|e\rangle$  of the transmon, respectively.

In the interaction picture under the Hamiltonian  $H_0$ , the effective Hamiltonian (8) changes to

$$\begin{aligned} H_e = & \left( \frac{g_A^2}{\Delta_A} a a^\dagger + \frac{g_B^2}{\Delta_B} b b^\dagger \right) |f\rangle\langle f| \\ & - \left( \frac{g_A^2}{\Delta_A} a^\dagger a + \frac{g_B^2}{\Delta_B} b^\dagger b \right) |e\rangle\langle e| \\ & + \mu \left( a^\dagger b e^{i\delta t} + a b^\dagger e^{-i\delta t} \right) (|f\rangle\langle f| - |e\rangle\langle e|), \end{aligned} \quad (9)$$

where  $\delta = \omega_A - \omega_B$ . Without loss of generality and for simplicity, we assume that  $\Delta_A = \Delta_B = \Delta$  (i.e.,  $\omega_A = \omega_B$ ) and  $g_A = g_B = g$ . Thus, the Hamiltonian (9) reduces to

$$\begin{aligned} H_e = & \chi (a a^\dagger + b b^\dagger) |f\rangle\langle f| - \chi (a^\dagger a + b^\dagger b) |e\rangle\langle e| \\ & + \mu (a^\dagger b + a b^\dagger) (|f\rangle\langle f| - |e\rangle\langle e|) \end{aligned} \quad (10)$$

with the dispersive shift  $\chi = g^2/\Delta$ . When the auxiliary level  $|f\rangle$  of transmon qubit is not occupied, the final effective Hamiltonian (10) can be written as

$$H_e = -\chi (a^\dagger a + b^\dagger b) |e\rangle\langle e| - \mu (a^\dagger b + a b^\dagger) |e\rangle\langle e|. \quad (11)$$

If we eliminate the degrees of freedom for the transmon qubit, the effective Hamiltonian  $H_e$  is exactly the standard Hamiltonian which describes the JC interaction between the cavities  $A$  and  $B$ .

#### IV. EXPERIMENTAL IMPLEMENTATION OF A QUANTUM ADDER IN 3D CIRCUIT QED

In this section we show how to prepare a superposition state for arbitrary input states. Let  $|\psi\rangle_A = \sum_{n=0}^{\infty} c_n |n\rangle_A$  and  $|\varphi\rangle_B = \sum_{m=0}^{\infty} d_m |m\rangle_B$  be two arbitrary input pure states of microwave cavities  $A$  and  $B$ , respectively. We assume that transmon qubit is in an arbitrary superposition state  $|\phi\rangle_T = \sin\theta|g\rangle + \cos\theta|e\rangle$ . Here, the Fock states of the cavities are expressed as  $|n\rangle_A = \frac{(a^\dagger)^n}{\sqrt{n!}}|0\rangle_A$  and  $|m\rangle_B = \frac{(b^\dagger)^m}{\sqrt{m!}}|0\rangle_B$ .

Under the Hamiltonian (11), the initial state of the total system  $|\phi\rangle_T |\psi\rangle_A |\varphi\rangle_B$  therefore evolves into

$$\sin\theta|g\rangle|\psi\rangle_A|\varphi\rangle_B + e^{iH'_0 t} e^{iH'_I t} \cos\theta|e\rangle|\psi\rangle_A|\varphi\rangle_B \quad (12)$$

where  $H'_0 = \chi(a^\dagger a + b^\dagger b)$ ,  $H'_I = \mu(a^\dagger b + a b^\dagger)$ , and we have used  $\langle g|e\rangle = 0$ .

By solving the Heisenberg equations for  $H'_I$ , the dynamics of the operators  $a^\dagger$  and  $b^\dagger$  can be derived as

$$\begin{aligned} a^\dagger(t) &= \cos(\mu t) a^\dagger + i \sin(\mu t) b^\dagger \\ b^\dagger(t) &= \cos(\mu t) b^\dagger + i \sin(\mu t) a^\dagger. \end{aligned} \quad (13)$$

For  $t = (\pi/2\mu)$ , one has  $a^\dagger(t) = i b^\dagger$  [ $a(t) = -i b$ ] and  $b^\dagger(t) = i a^\dagger$  [ $b(t) = -i a$ ]. That corresponds to a exchange of quantum states between two microwave cavities except for a phase shift  $3\pi/2$ . When the evolution time  $t = (\pi/2\mu)$ , the Eq. (12) changes to

$$\sin\theta|g\rangle|\psi\rangle_A|\varphi\rangle_B + \cos\theta|e\rangle|\varphi\rangle_A|\psi\rangle_B, \quad (14)$$

where we have used  $a^\dagger a |n\rangle = n |n\rangle$ ,  $b^\dagger b |m\rangle = m |m\rangle$ ,  $(i)^n = e^{in\pi(2k+1/2)}$ , and  $(i)^m = e^{im\pi(2k+1/2)}$  with  $k$  an integer. It should be noted that when the evolution time  $t = (\pi/2\mu)$ , the additional phase shifts can be completely dropped by taking into account the photon-number-dependent shifts with Hamiltonian  $H'_0$ .

We perform a  $-\pi/2$  rotation on the transmon qubit that realizes the conversions  $|g\rangle \rightarrow |+\rangle$  and  $|e\rangle \rightarrow |-\rangle$  with  $|+\rangle = (|e\rangle + |g\rangle)/\sqrt{2}$  and  $|-\rangle = (|e\rangle - |g\rangle)/\sqrt{2}$ . Now we perform a projective measurement onto the state  $|+\rangle$  or  $|-\rangle$  of transmon qubit, the state (14) becomes

$$\cos\theta|\varphi\rangle_A|\psi\rangle_B \pm \sin\theta|\psi\rangle_A|\varphi\rangle_B. \quad (15)$$

Then we perform another measurement on the cavity  $B$  in the referential state  $|\chi\rangle_B$  that satisfies  $\langle\chi|\psi\rangle_B \neq 0$  and  $\langle\chi|\varphi\rangle_B \neq 0$ . Thus, one can obtain the following superposition state of cavity  $A$

$$|\Psi\rangle_A = \frac{1}{N}(\eta|\varphi\rangle \pm \gamma|\psi\rangle), \quad (16)$$

where  $\gamma = \sin\theta\langle\chi|\varphi\rangle_B$ ,  $\eta = \cos\theta\langle\chi|\psi\rangle_B$ , and  $N = \sqrt{2[|\gamma|^2 + |\eta|^2 \pm 2\text{Re}(\gamma\eta^*\langle\varphi|\psi\rangle)]}$ . Here, the sign  $+$  or  $-$  of the output state conditioning on the measurement  $|+\rangle$  or  $|-\rangle$  of transmon qubit. It can be seen that the performance of the above superposition state is possible with prior knowledge of the overlaps of  $\langle\chi|\varphi\rangle$  and  $\langle\chi|\psi\rangle$ .

## V. POSSIBLE EXPERIMENTAL IMPLEMENTATION

Recent experimental results for the 3D circuit system demonstrate the great promise of quantum computation and QIP. For an experimental implementation, our setup of two superconducting 3D cavities coupled to a transmon has been demonstrated recently by [35].

Taking into account the effect of the dissipation and the dephasing of system, the dynamics of the lossy system is governed by the Markovian master equation

$$\begin{aligned} \frac{d\rho}{dt} = & -i[H, \rho] + \kappa_A \mathcal{D}[a] + \kappa_B \mathcal{D}[b] \\ & + \gamma_{eg} \mathcal{D}[\sigma_{eg}^-] + \gamma_{fe} \mathcal{D}[\sigma_{fe}^-] + \gamma_{fg} \mathcal{D}[\sigma_{fg}^-] \\ & + \gamma_{\varphi e} \mathcal{D}[\sigma_{ee}^-] + \gamma_{\varphi f} \mathcal{D}[\sigma_{ff}^-], \end{aligned} \quad (17)$$

where  $\rho$  is the density matrix of the whole system,  $H$  is given by Eqs. (3) and (4),  $\sigma_{fg}^- = |g\rangle\langle f|$ ,  $\sigma_{ee}^- = |e\rangle\langle e|$ ,  $\sigma_{ff}^- = |f\rangle\langle f|$ , and  $\mathcal{D}[\mathcal{O}] = (2\mathcal{O}\rho\mathcal{O}^\dagger - \mathcal{O}^\dagger\mathcal{O}\rho - \rho\mathcal{O}^\dagger\mathcal{O})/2$  is the dissipator. Here,  $\kappa_A$  ( $\kappa_B$ ) is the decay rate of cavity  $A$  ( $B$ ). In addition,  $\gamma_{eg}$ ,  $\gamma_{fe}$ , and  $\gamma_{fg}$  are the energy relaxation rates from state  $|e\rangle$  to  $|g\rangle$ ,  $|f\rangle$  to  $|e\rangle$ , and  $|f\rangle$  to  $|g\rangle$  of transmon qubit, respectively.  $\gamma_{\varphi e}$  ( $\gamma_{\varphi f}$ ) is the dephasing rate of the level  $|e\rangle$  ( $|f\rangle$ ) of transmon qubit.

The generation efficiency can be evaluated by fidelity  $\mathcal{F} = \sqrt{\langle \psi_{\text{id}} | \rho | \psi_{\text{id}} \rangle}$ , where  $|\psi_{\text{id}}\rangle$  is the ideal target state given in Eq. (14). In addition, the input state of the transmon-cavity system is  $(\sin\theta|g\rangle + \cos\theta|e\rangle)|\psi\rangle_A|\varphi\rangle_B$ . The initial state of cavities  $|\psi\rangle_A$  and  $|\varphi\rangle_B$  can be arbitrary states such as discrete-variable states or continuous-variable states. In the following, we choose the cavities are initially in the coherent states, i.e.,  $|\psi\rangle_A = |\alpha\rangle_A$  and  $|\varphi\rangle_B = |-\beta\rangle_B$  with  $\alpha = \beta = 0.1$ .

We now numerically simulate the fidelity of the operation by solving the master equation (17). Since the transmon qubit relaxation time  $T_1 = 75 \mu\text{s}$ , the transmon qubit dephasing time  $T_2 = 45 \mu\text{s}$ , and the cavity relaxation time  $T_1 = 3.3 \text{ ms}$  have been achieved in similar 3D circuit system [35], we set  $\gamma_{\varphi e}^{-1} = 15 \mu\text{s}$ ,  $\gamma_{\varphi f}^{-1} = 10 \mu\text{s}$ ,  $\gamma_{eg}^{-1} = 50 \mu\text{s}$ ,  $\gamma_{fe}^{-1} = 25 \mu\text{s}$ ,  $\gamma_{fg}^{-1} = 100 \mu\text{s}$ ,  $\kappa_A^{-1} = 15 \mu\text{s}$ ,  $\kappa_B^{-1} = 10 \mu\text{s}$ .

Figure 3 shows the fidelity  $\mathcal{F}$  versus the dispersive shift  $\chi = g^2/\Delta$ . Without loss of generality, we here choose  $\sin\theta = \cos\theta = 1/\sqrt{2}$ . The red squares depicted in Fig. 3 show that for  $\chi \geq 1 \text{ MHz}$ , the operational fidelity based on the original Hamiltonian  $H_I$  can be greater than 97.80%. We also calculate the operational fidelity using the effective Hamiltonian  $H_e$ , as shown in Fig. 3 for the blue squares. The blue squares display that compared to the use of the effective Hamiltonian, the fidelity is almost unchanged. This indicates that the approximation made for the effective Hamiltonian is reasonable. According to Ref. [35], we choose  $\Delta = 0.7 \text{ GHz}$  in our numerical simulation. In the following, we choose the dispersive shift  $\chi = 1 \text{ MHz}$  that because this value of  $\chi$  is readily avail-

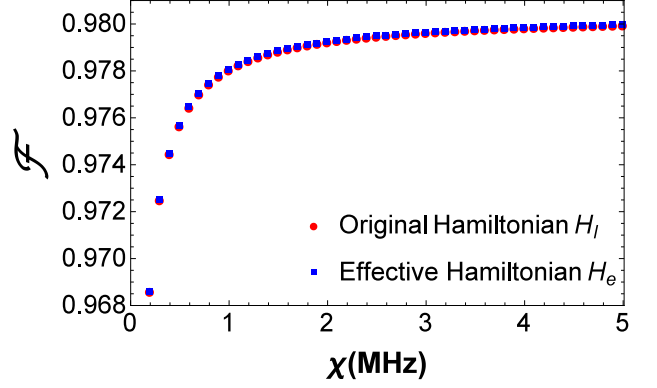


FIG. 3: (color online) Fidelity  $\mathcal{F}$  versus the dispersive shift  $\chi = g^2/\Delta$ . The parameters used in the numerical simulation are given in the main text.

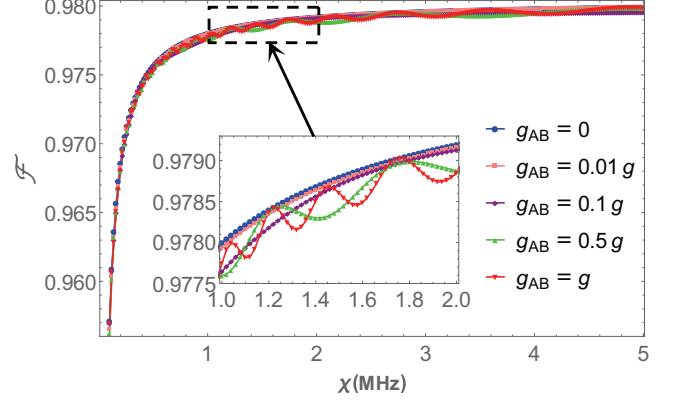


FIG. 4: (color online) Fidelity  $\mathcal{F}$  versus the  $\chi = g^2/\Delta$  and by taking the unwanted inter-cavity crosstalk into account.

able in experiments [35]. Moreover, the coupling strength  $g$  can be calculated from the  $\chi$ .

To investigate the effect of the undesired inter-cavity crosstalk on the fidelity, we numerically calculate the operation fidelity with the crosstalk between two cavities in Fig. 4. The effect of the inter-cavity crosstalk can be taken into account by adding a Hamiltonian of the form  $H_{AB} = g_{AB}(a^\dagger b + ab^\dagger)$  in  $H_I$ , where  $g_{AB}$  is the inter-cavity crosstalk coupling strength. Figure 4 shows fidelity  $\mathcal{F}$  versus  $\chi$  for  $g_{AB} = 0, 0.01g, 0.1g, 0.5g, g$ . These the coupling strength conditions are easily satisfied by the present circuit QED technology [43]. From the Fig. 4 one can see that the crosstalk effect is very small or negligible for  $g_{AB} \leq 0.1g$ . It is interesting to note that for  $g_{AB} = 0.5g, g$ , the effect of the crosstalk error on the fidelity is negligibly small for some green and red data points. The parameters used here are referred to Fig. 3.

Figure 5 shows output fidelities from the master equation simulation, which takes into account the inhom-

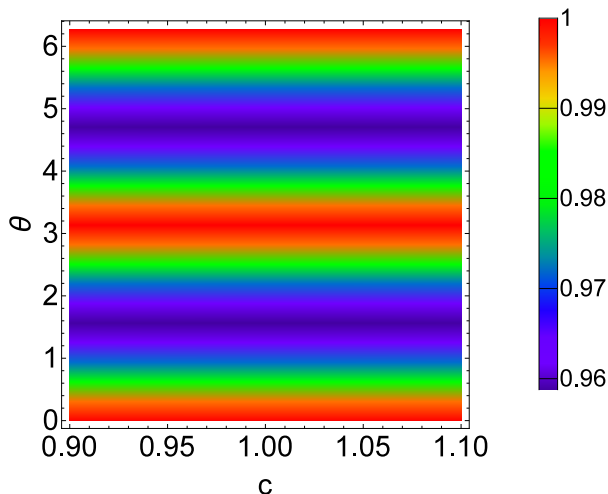


FIG. 5: (color online) Fidelity  $\mathcal{F}$  versus  $c$  and  $\theta$ . Here  $g_A = g$  and  $g_B = cg$  with  $c \in [0.9, 1.1]$ .

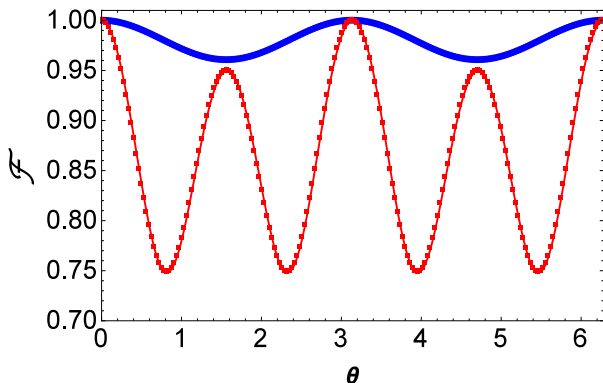


FIG. 6: (color online) Fidelity  $\mathcal{F}$  versus  $\theta$ , which is plotted by choosing  $\chi = 1$  MHz.

geneity in transmon-cavity interaction and the possibility of choosing a number of initial states of transmon. Figure 5 displays the fidelity versus  $c$  and  $\theta$ , where we set  $g_A = g$  and  $g_B = cg$  with  $c \in [0.9, 1.1]$ . We can see from this figure that with the change of the  $c$ , the fidelity is almost unaffected in the regions  $0.9 \leq c < 1$  and  $1 < c \leq 1.1$ . That means the coupling strengths  $g_A$  and  $g_B$  are not necessarily strictly equal in our proposal. From Fig. 5, the average fidelity is about 97.80% for  $\theta \in [0, 2\pi]$ . Moreover, the fidelity is above 99.95% for all  $c$  for  $\theta = 0.1\pi, 1.1\pi$  and  $1.9\pi$ .

Due to the weak anharmonicity of the transmon, we further consider the error induced by unwanted interaction between cavity  $j$  ( $j = A, B$ ) and  $|g\rangle \leftrightarrow |e\rangle$  transition of transmon, which is described by the Hamiltonian

$$\widetilde{H}_I = (g/\sqrt{2})(a\sigma_{eg}^+ e^{i\delta t} + a^\dagger \sigma_{eg}^-) + (g/\sqrt{2})(b\sigma_{eg}^+ + b^\dagger \sigma_{eg}^-).$$

Here, we take the detuning  $\delta = \omega_{eg} - \omega_j$  with  $j = A, B$ . For a transmon qubit, the transition between levels  $|g\rangle$  and  $|f\rangle$  is forbidden or very weak [44]. Thus, the couplings of the cavities with the transition  $|g\rangle \leftrightarrow |f\rangle$  can be neglected.

We have considered the effect of the weak anharmonicity error on the operational fidelity, by adding the term  $\widetilde{H}_I$  to the  $H_I$ , as the red and blue curves shown in Fig. 6. Figure 6 displays the fidelity  $\mathcal{F}$  versus the  $\theta$  with  $\theta \in [0, 2\pi]$ . The blue curve shown in Fig. 6 corresponds to the case of no weak anharmonicity error, while the red curve corresponds to the case that the weak anharmonicity error is taken into account. One finds that the fidelity is almost unaffected by the weak anharmonicity error for  $\theta = 0.5\pi, 1.05\pi$  and  $1.5\pi$ .

The simulations above show that the quantum adder that generates a superposition of two unknown states with high fidelity can be achieved for small errors in the undesired inter-cavity crosstalk, the weak anharmonicity, and the inhomogeneity.

## VI. CONCLUSION

We have devised a quantum adder based on 3D circuit QED that is a good candidate for quantum information processing, computation and simulation. The 3D microwave cavities dispersively interacting with the transmon to effectively create a superposition state of two arbitrary states encoded in two cavities. The initial state of each cavity is arbitrarily that selected as the discrete-variable state or the continuous-variable state. Our proposal also can be applied to other types of qubits such as natural atoms [38] and artificial atoms (other superconducting qubits (e.g., phase qubits [39], Xmon qubits [40], flux qubit [41]), NV centers [42], and quantum dots [37]). The Numerical simulations imply that the high-fidelity generation of a superposition state of two cavities is feasible with the current circuit QED technology. Finally, our proposal provides a way for realizing a quantum adder in a 3D circuit QED system, and such quantum machine may find other applications in quantum information processing and computation. We hope this work would stimulate experimental activities in the near future.

## ACKNOWLEDGEMENTS

This work was supported by the National Natural Science Foundation of China, under Grant No.11775040 and No. 11375036, and the Fundamental Research Fund for the Central Universities under Grants No. DUT18LK45.

- 
- [1] R. Horodecki, P. Horodecki, M. Horodecki, and K. Horodecki, Quantum entanglement, *Rev. Mod. Phys.* **81**, 865 (2009).
- [2] T. Baumgratz, M. Cramer, and M. B. Plenio, Quantifying coherence, *Phys. Rev. Lett.* **113**, 140401 (2014).
- [3] C. S. Yu, Quantum coherence via skew information and its polygamy, *Phys. Rev. A* **95**, 042337 (2017).
- [4] P. W. Shor, Polynomial-time algorithms for prime factorization and discrete logarithms on a quantum computer, *SIAM J. Comput.* **26**, 1484 (1997).
- [5] L. K. Grover, A fast quantum mechanical algorithm for database search, in *Proceedings of the Twenty-Eighth Annual ACM Symposium on Theory of Computing* (ACM Press, New York, 1996), pp. 212-219.
- [6] V. Giovannetti, S. Lloyd, and L. Maccone, Advances in quantum metrology, *Nat. Photonics* **5**, 222 (2011).
- [7] N. Gisin, G. Ribordy, W. Tittel, and H. Zbinden, Quantum cryptography, *Rev. Mod. Phys.* **74**, 745 (2002).
- [8] Y. Alvarez-Rodriguez, M. Sanz, L. Lamata, and E. Solano, The forbidden quantum adder, *Sci. Rep.* **5**, 11983 (2015).
- [9] M. Oszmaniec, A. Grudka, M. Horodecki, and A. Wójcik, Creating a superposition of unknown quantum states, *Phys. Rev. Lett.* **116**, 110403 (2016).
- [10] M. Doosti, F. Kianvash, and V. Karimipour, Universal superposition of orthogonal states, *Phys. Rev. A* **96**, 052318 (2017).
- [11] G. Gatti, D. Barberena, M. Sanz, and E. Solano, Protected state transfer via an approximate quantum adder, *Sci. Rep.* **7**, 6964 (2017).
- [12] X. M. Hu, M. J. Hu, J. S. Chen, B. H. Liu, Y. F. Huang, C. F. Li, G. C. Guo, and Y. S. Zhang, Experimental creation of superposition of unknown photonic quantum states, *Phys. Rev. A* **94**, 033844 (2016).
- [13] K. Li, G. Long, H. Katiyar, T. Xin, G. Feng, D. Lu, and R. Laflamme, Experimentally superposing two pure states with partial prior knowledge, *Phys. Rev. A* **95**, 022334 (2017).
- [14] J. Q. You and F. Nori, Atomic physics and quantum optics using superconducting circuits, *Nature* **474**, 589 (2011).
- [15] M. H. Devoret and R. J. Schoelkopf, Superconducting circuits for quantum information: An outlook, *Science* **339**, 1169 (2013).
- [16] X. Gu, A. F. Kockum, A. Miranowicz, Y. X. Liu, and F. Nori, Microwave photonics with superconducting quantum circuits, *Physics Reports* **718**, 1 (2017).
- [17] A. Romanenko, R. Pilipenko, S. Zorzetti, D. Frolov, M. Awida, S. Posen, and A. Grassellino, Three-dimensional superconducting resonators at  $T < 20$  mK with the photon lifetime up to  $\tau = 2$  seconds, arXiv:1810.03703 (2018).
- [18] C. Rigetti, J. M. Gambetta, S. Poletto, B. L. T. Plourde, J. M. Chow, A. D. Córcoles, J. A. Smolin, S. T. Merkel, J. R. Rozen, G. A. Keefe, M. B. Rothwell, M. B. Ketchen, and M. Steffen, Superconducting qubit in a waveguide cavity with a coherence time approaching 0.1 ms, *Phys. Rev. B* **86**, 100506(R) (2012).
- [19] M. Mariantoni, F. Deppe, A. Marx, R. Gross, F. K. Wilhelm, and E. Solano, Two-resonator circuit quantum electrodynamics: A superconducting quantum switch, *Phys. Rev. B* **78**, 104508 (2008).
- [20] S. T. Merkel and F. K. Wilhelm, Generation and detection of NOON states in superconducting circuits, *New J. Phys.* **12**, 093036 (2010).
- [21] F. W. Strauch, K. Jacobs, and R. W. Simmonds, Arbitrary control of entanglement between two superconducting resonators, *Phys. Rev. Lett.* **105**, 050501 (2010).
- [22] S. J. Xiong, Z. Sun, J. M. Liu, T. Liu, and C. P. Yang, Efficient scheme for generation of photonic NOON states in circuit QED, *Opt. Lett.* **40**, 2221 (2015).
- [23] R. Sharma and F. W. Strauch, Quantum state synthesis of superconducting resonators, *Phys. Rev. A* **93**, 012342 (2016).
- [24] Y. J. Zhao, C. Q. Wang, X. B. Zhu, and Y. X. Liu, Engineering entangled microwave photon states through multiphoton interactions between two cavity fields and a superconducting qubit, *Sci. Rep.* **6** 23646 (2016).
- [25] Q. P. Su, H. H. Zhu, L. Yu, Y. Zhang, S. J. Xiong, J. M. Liu, and C. P. Yang, Generating double NOON states of photons in circuit QED, *Phys. Rev. A* **95**, 022339 (2017).
- [26] T. Liu, B. Q. Guo, C. S. Yu, and W. N. Zhang, One-step implementation of a hybrid Fredkin gate with quantum memories and single superconducting qubit in circuit QED and its applications, *Opt. Express* **26** 4498 (2018).
- [27] C. P. Yang, Q. P. Su, and S. Han, Generation of Greenberger-Horne-Zeilinger entangled states of photons in multiple cavities via a superconducting qutrit or an atom through resonant interaction, *Phys. Rev. A* **86**, 022329 (2012).
- [28] T. Liu, Q. P. Su, S. J. Xiong, J. M. Liu, C. P. Yang, and F. Nori, Generation of a macroscopic entangled coherent state using quantum memories in circuit QED. *Sci. Rep.* **6**, 32004 (2016).
- [29] T. Liu, Y. Zhang, B. Q. Guo, C. S. Yu, and W. N. Zhang, Circuit QED: cross-Kerr effect induced by a superconducting qutrit without classical pulses, *Quantum Inf. Process.* **16**, 209 (2017).
- [30] H. Zhang, A. Alsaedi, T. Hayat, and F. G. Deng, Entanglement concentration and purification of two-mode squeezed microwave photons in circuit QED, *Annals of Physics* **391**, 112 (2018).
- [31] H. Paik, D. I. Schuster, L. S. Bishop, G. Kirchmair, G. Catelani, A. P. Sears, B. R. Johnson, M. J. Reagor, L. Frunzio, L. I. Glazman, S. M. Girvin, M. H. Devoret, and R. J. Schoelkopf, Observation of high coherence in Josephson junction qubits measured in a three-dimensional circuit QED architecture, *Phys. Rev. Lett.* **107**, 240501 (2011).
- [32] B. Vlastakis, G. Kirchmair, Z. Leghtas, S. E. Nigg, L. Frunzio, S. M. Girvin, M. Mirrahimi, M. H. Devoret, R. J. Schoelkopf, Deterministically encoding quantum information using 100-photon Schrödinger cat states, *Science* **342**, 607 (2013).
- [33] M. J. Peterer, S. J. Bader, X. Jin, F. Yan, A. Kamal, T. J. Gudmundsen, P. J. Leek, T. P. Orlando, W. D. Oliver, and S. Gustavsson, Coherence and decay of higher energy levels of a superconducting transmon qubit, *Phys. Rev. Lett.* **114**, 010501 (2015).
- [34] N. Ofek, A. Petrenko, R. Heeres, P. Reinhold, Z. Leghtas, B. Vlastakis, Y. Liu, L. Frunzio, S. M. Girvin, L. Jiang, M. Mirrahimi, M. H. Devoret, and R. J. Schoelkopf, Ex-

- tending the lifetime of a quantum bit with error correction in superconducting circuits, *Nature* **536**, 441 (2016).
- [35] C. Wang, Y. Y. Gao, P. Reinhold, R. W. Heeres, N. Ofek, K. Chou, C. Axline, M. Reagor, J. Blumoff, K. M. Sliwa, L. Frunzio, S. M. Girvin, L. Jiang, M. Mirrahimi, M. H. Devoret, R. J. Schoelkopf, A Schrödinger cat living in two boxes, *Science* **352**, 1087 (2016).
- [36] S. Rosenblum, Y. Y. Gao, P. Reinhold, C. Wang, C. J. Axline, L. Frunzio, S. M. Girvin, L. Jiang, M. Mirrahimi, M. H. Devoret, and R. J. Schoelkopf, A CNOT gate between multiphoton qubits encoded in two cavities, *Nature Comm.* **9**, 652 (2018).
- [37] K. Hennessy, A. Badolato, M. Winger, D. Gerace, M. Atatüre, S. Gulde, S. Fält, E. L. Hu, and A. Imamoglu, Quantum nature of a strongly coupled single quantum dot-cavity system, *Nature* **445**, 896 (2007).
- [38] K. M. Birnbaum, A. Boca, R. Miller, A. D. Boozer, T. E. Northup, and H. J. Kimble, Photon blockade in an optical cavity with one trapped atom, *Nature* **436**, 87 (2005).
- [39] H. Wang, M. Mariantoni, R. C. Bialczak, M. Lenander, E. Lucero, M. Neeley, A. D. O'Connell, D. Sank, M. Weides, J. Wenner, T. Yamamoto, Y. Yin, J. Zhao, J. M. Martinis, and A. N. Cleland, *Phys. Rev. Lett.* **106**, 060401 (2011).
- [40] R. Barends, J. Kelly, A. Megrant, D. Sank, E. Jeffrey, Y. Chen, Y. Yin, B. Chiaro, J. Mutus, C. Neill, P. O'Malley, P. Roushan, J. Wenner, T. C. White, A. N. Cleland, and J. M. Martinis, Coherent josephson qubit suitable for scalable quantum integrated circuits, *Phys. Rev. Lett.* **111**, 080502 (2013).
- [41] F. Yan, S. Gustavsson, A. Kamal, J. Birenbaum, A. P. Sears, D. Hover, T. J. Gudmundsen, D. Rosenberg, G. Samach, S. Weber, J. L. Yoder, T. P. Orlando, J. Clarke, A. J. Kerman, and W. D. Oliver, The flux qubit revisited to enhance coherence and reproducibility, *Nature Commun.* **7**, 12964 (2016).
- [42] X. Zhu, S. Saito, A. Kemp, K. Kakuyanagi, S. Karimoto, H. Nakano, W. J. Munro, Y. Tokura, M. S. Everitt, K. Nemoto, M. Kasu, N. Mizuochi, and K. Semba, Coherent coupling of a superconducting flux qubit to an electron spin ensemble in diamond, *Nature* **478**, 221 (2011).
- [43] T. Liu, X. Z. Cao, Q. P. Su, S. J. Xiong, and C. P. Yang, Multi-target-qubit unconventional geometric phase gate in a multi-cavity system, *Sci. Rep.* **6**, 21562 (2016).
- [44] J. Koch, T. M. Yu, J. Gambetta, A. A. Houck, D. I. Schuster, J. Majer, A. Blais, M. H. Devoret, S. M. Girvin, and R. J. Schoelkopf, Charge-insensitive qubit design derived from the Cooper pair box, *Phys. Rev. A* **76**, 042319 (2007).